

# Sub-Femtosecond Stark Control of Molecular Photoexcitation with Near Single-Cycle Pulses

Benoit Mignolet,<sup>\*,†</sup> Basile F. E. Curchod,<sup>‡</sup> Françoise Remacle,<sup>†</sup> and Todd J. Martínez<sup>\*,§,||</sup>

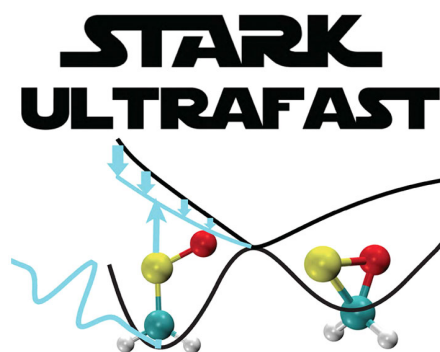
<sup>†</sup>Theoretical Physical Chemistry, Research Unit Molecular Systems, B6c, University of Liège, B4000 Liège, Belgium

<sup>‡</sup>Department of Chemistry, Durham University, South Road, Durham DH1 3LE, United Kingdom

<sup>§</sup>Department of Chemistry and the PULSE Institute, Stanford University, 333 Campus Drive, Stanford, California 94305, United States

<sup>||</sup>SLAC National Accelerator Laboratory, 2575 Sand Hill Road, Menlo Park, California 94025, United States

**ABSTRACT:** Electric fields can tailor molecular potential energy surfaces by interaction with the electronic state-dependent molecular dipole moment. Recent developments in optics have enabled the creation of ultrashort few-cycle optical pulses with precise control of the carrier envelope phase (CEP) that determines the offset of the maxima in the field and the pulse envelope. This opens new ways of controlling ultrafast molecular dynamics by exploiting the CEP. In this work, we show that the photoabsorption efficiency of oriented H<sub>2</sub>CSO (sulfine) can be controlled by tuning the CEP. We further show that this control emanates from a resonance condition related to Stark shifting of the electronic energy levels.



Potential energy surfaces (PESs) are the foundation for the familiar picture of reaction energies, reaction barriers, and excitation energies. Many chemical strategies for enhancing reactivity, such as catalysis or functional group substitution, alter the shape and/or topology of the relevant PES by lowering energy barriers along the reaction path. In principle, one can also accomplish such changes with electric fields, originating from the molecular environment<sup>1–3</sup> or from electromagnetic radiation.<sup>4</sup> Electric fields interact with the molecular charge density, influencing the energy of electronic states. An approximate but nevertheless useful and intuitive picture focuses on the interaction of the field with permanent molecular dipole moments, i.e., the Stark effect. The Stark effect has been used to control the ionization yield<sup>5</sup> or the outcome of a chemical reaction by dynamical laser-induced modification of potential energy barriers, as shown for the photodissociation of IBr.<sup>4,6</sup> Stark-based control is based on the orientation of the electric field with respect to the molecule, stabilizing/destabilizing electronic states with dipole moments parallel/antiparallel to the electric field. When a typical femtosecond (or longer) pulse containing a large number of electric field oscillations is applied to a molecule, the electronic energy is raised and lowered in each cycle and the effect is often averaged out. However, recent progress in molecular orientation<sup>7–9</sup> and generation of ultrashort near single-cycle pulses<sup>10–12</sup> promises to enable the application of pulses where the electric field has a specific molecular-frame orientation when it most strongly interacts with the molecule (i.e., at the

maximum of the pulse envelope), opening new avenues for the control of chemical reactivity by tuning the PES and selectively lowering or raising reaction barriers.

The term “ultrashort pulse” can imply (i) that the pulse duration is short, typically on the attosecond time scale,<sup>13,14</sup> or (ii) that the pulse contains only one or few oscillations of the electric field within its envelope, therefore reaching its intrinsic temporal limit.<sup>15–17</sup> Single-cycle or near single-cycle pulses have been generated across the electromagnetic spectrum, ranging from IR<sup>18–20</sup> to VUV<sup>21</sup> and XUV<sup>14</sup> regions. Because there are very few oscillations of the electric field during the pulse duration, the phase between the electric field and the envelope, known as the carrier-envelope phase (CEP), can strongly affect the ensuing dynamics.<sup>22–25</sup> Depending on the CEP, the electric field at the maximum of the pulse envelope (when the light–matter interaction is maximal) can be either positive or negative (Figure 1). Previous demonstrations of the effect of CEP using few-cycle IR pulses include dissociative ionization of H<sub>2</sub><sup>26</sup>/D<sub>2</sub><sup>27</sup> and other diatomic molecules,<sup>28–30</sup> control of proton migration,<sup>31</sup> deprotonation,<sup>32</sup> or fragmentation pathways<sup>33</sup> of hydrocarbons, and control of the electronic density of C<sub>60</sub>.<sup>34</sup> Most of the experiments with CEP control take place in cationic states, or the resulting dynamics is probed by photoionization. Little attention has been paid to

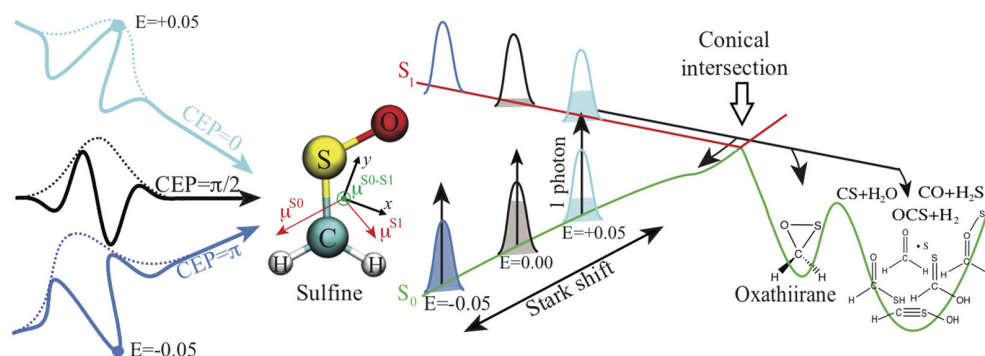


**Figure 1.** Schematic view of the  $S_0$ – $S_1$  photoexcitation of the  $\text{H}_2\text{CSO}$  sulfine and its ensuing photochemistry. The molecule is planar and oriented according to the moment of inertia, with the  $z$  axis (pointing out of the page) corresponding to the inertia eigenvector perpendicular to the molecular ( $x$ – $y$ ) plane. Under illumination by an electric field, the  $S_0 \rightarrow S_1$  excitation energy increases for a field polarized in the  $-x$  direction due to the Stark shift effect, and it decreases for a field polarized in the  $+x$  direction. The permanent dipole moments of the  $S_0$  and  $S_1$  states ( $\mu^{S_0}$  and  $\mu^{S_1}$ ) have nonvanishing components only in the ( $x$ ,  $y$ ) plane. They are shown along with the  $S_0$ – $S_1$  transition dipole moment ( $\mu^{S_0-S_1}$ ), which is perpendicular to the molecular plane. The Gaussians represent the wavepacket and the filling corresponds to the population in  $S_0$  and  $S_1$  after application of the pulse. All the pulses used for the photoexcitation have the same parameters ( $f_0 = 0.07\text{au}$ ,  $\text{fwhm} = 1.7\text{ fs}$ ,  $\omega = 0.063\text{ au}$ ) except for the CEP that varies between 0 and  $2\pi$  and the polarization that varies between  $0^\circ$  and  $45^\circ$  in the  $z$ – $x$  plane.

possible applications of CEP control in neutral molecules. Dynamical simulations highlighted the CEP effect on purely electronic dynamics (i.e., with frozen nuclei) of diatomic<sup>25,35</sup> and polyatomic neutral molecules<sup>36</sup> as well as on the fragmentation and ionization<sup>37</sup> yield including nuclei motion.<sup>38</sup> During the pulse, the excitation energies are modified by the interaction between the electronic states and the electric field of the pulse, which depends on its waveform and so its CEP.<sup>39</sup> This results in a nonequilibrium electronic density that subsequently couples to the nuclear motion.

Single-cycle or near single-cycle pulses can be used to tailor the PES of the ground ( $S_0$ ) and excited ( $S_x$ ) states of neutral molecules. During the pulse, the PESs are dynamically modified by interaction with the electric field  $\mathbf{E}(t)$ . For oriented molecules, this gives rise to a time-dependent excitation energy between  $S_0$  and  $S_x$  that can be expressed in first-order perturbation theory (Stark effect) as  $\Delta E_{S_0-S_x}^{\text{field-induced}}(t) = \Delta E_{S_0-S_x}^{\text{field-free}} - \Delta \mu_{S_0-S_x} \cdot \mathbf{E}(t)$ . The field-free excitation energy is modulated by the dot product of  $\mathbf{E}(t)$  with the difference of permanent dipole moments on the two electronic states:  $\Delta \mu_{S_0-S_x} = (\mu_{S_x} - \mu_{S_0})$ . This expression for the field-induced excitation energy is solely based on the Stark effect and provides an intuitive picture provided that the electronic density rapidly adapts to the field strength, which is most appropriate for “slow” IR pulses.<sup>39</sup> It should be noted that the electric field can also mix electronic states through their transition dipole moments (see Supporting Information) and that for fast oscillating pulses, the behavior of the electronic density is less adiabatic with respect to the field.<sup>39</sup>

Depending on  $\mathbf{E}(t)$  and the CEP, the Stark shift will either increase or decrease the adiabatic excitation energy of oriented molecules (see Figure 1), and the extent of this effect will depend on the laser intensity. Because the transfer of population is largest at the maximum of the pulse envelope, we focus on the Stark shift and excitation energy at this time. Control over molecular excitation could be achieved by matching the adiabatic excitation energy at the maximum of the pulse envelope to the carrier wavelength of the pulse. As near-single-cycle pulses have short duration, they are broad in energy (see Figure 2a), making the photoexcitation possible for a range of frequencies. The transfer of population will be larger

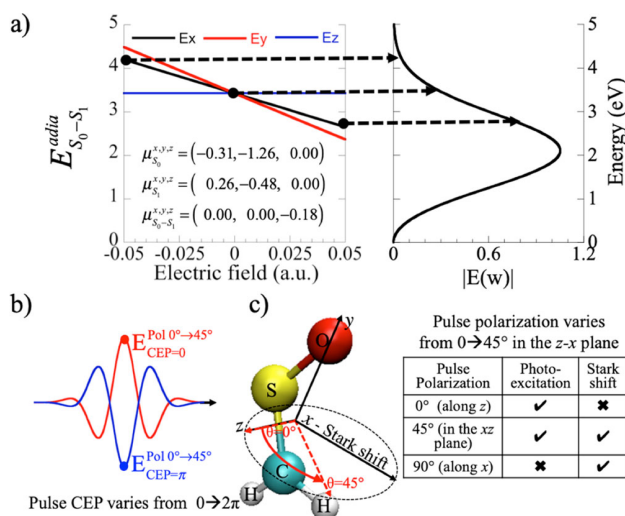


**Figure 2.** (a) Adiabatic  $S_0 \rightarrow S_1$  excitation energy computed at the SA2-CASSCF(4/3)/6-31G(d) level under illumination by a constant electric field polarized along  $x$ ,  $y$ , and  $z$  in the molecular frame. The values of the permanent and transition dipole moments of  $S_0$  and  $S_1$  are shown in the inset and the Fourier transform of the pulse  $\mathbf{E}(t)$  is shown on the left. (b) Pulse used in the simulations, with CEP tuned from 0 to  $2\pi$ . (c) To emphasize the role of the Stark shift on the CEP effect, the pulse polarization is varied, starting from a polarization along the  $z$  direction (no Stark shift) to a polarization in the  $z$ – $x$  plane (strong Stark effect).

for the CEP that matches the excitation energy of an optically bright state with the carrier wavelength. For other values of the CEP, the adiabatic excitation energy will be strongly off-resonant, leading to a decreased population transfer (Figure 1). This control could be applied to a wide range of molecules or molecular systems with permanent dipole moments. It is best achieved with incident frequencies that are off-resonant with respect to the field-free excitation energy, since the key idea is that the Stark shift brings the carrier frequency and the excitation energy into resonance. Controlling molecular excitations would enable short-pulse shaping of the PES, which could eventually be used to dynamically tailor reaction barriers in addition to photoabsorption efficiencies.

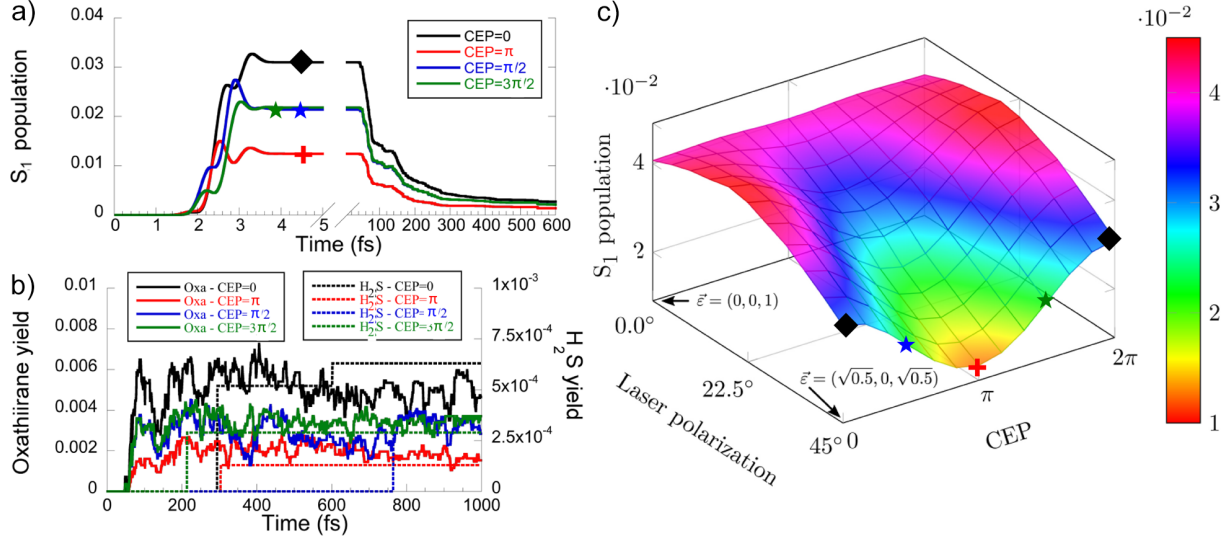


**Figure 3.** (a)  $S_1$  population during the excitation by a short IR pulse polarized at  $45^\circ$  in the  $x$ - $z$  polarization plane ( $f_0 = 0.07\text{au}$ ,  $\text{fwhm} = 1.7\text{ fs}$ ,  $\omega = 0.063\text{au}$ ,  $\epsilon = (1/\sqrt{2}, 0, 1/\sqrt{2})$ ) for CEP =  $0$ ,  $\pi/2$ ,  $\pi$ , and  $3\pi/2$ . (b) Yield of oxathirane and  $\text{H}_2\text{S}$  following photoexcitation by the IR pulse. (c)  $S_1$  population at the end of the pulse computed as a function of the CEP and laser polarization ranging from  $0^\circ$  to  $45^\circ$  in the  $z$ - $x$  polarization plane. The  $S_1$  populations from panel a are also noted with symbols.

We now discuss how the CEP in a near-single-cycle pulse can control molecular excitation. We model photoexcitation of an oriented ground-state sulfine<sup>40,41</sup> ( $\text{H}_2\text{CSO}$ ) molecule to its lowest excited state ( $S_1$ ) for a series of pulses with different CEP. Sulfine represents an ideal case for investigating CEP control because its  $S_0/S_1$  transition dipole moment is perfectly perpendicular to the  $S_0$  and  $S_1$  dipole moments (see Figure 1). This allows us to use the laser polarization to separate the excitation from the Stark effect. This property originates from the symmetry of the molecule that is planar and belongs to the  $C_s$  point group. The  $S_0$  and  $S_1$  ( $n \rightarrow \pi^*$  transition) states respectively belong to  $A'$  (totally symmetric) and  $A''$  irreducible representations, which implies that their permanent dipole moments perpendicular to the molecular plane (along  $z$ ) are zero and that the photoexcitation of the  $S_1$  state is only optically allowed for light polarized along  $z$ . The  $z$  component of the transition dipole moment is relatively small ( $-0.18\text{ au}$ ) due to the excitation of the nonbonding HOMO orbital to a  $\pi^*$  orbital in the  $S_1$  state. On the basis of the permanent dipole moments of the ground and excited states (Figure 2a), sulfine has an adiabatic excitation energy almost resonant (i.e., within the envelope of the pulse's Fourier transform) with a near-single-cycle 1.7 fs pulse polarized along the  $+x$  direction with a laser intensity of  $8.8 \times 10^{13}\text{ W/cm}^2$  (0.05 au; see Figure 2a) and a carrier wavelength of 720 nm as in ref 34. We computed the excited-state population for photoexcitation by this pulse with different values of the CEP (varied from 0 to  $2\pi$ ). To emphasize the effect of the Stark shift, we also varied the pulse polarization from a pulse completely polarized along  $z$  (when photoexcitation occurs without any Stark effect) to a pulse polarized in the  $z$ - $x$  polarization plane (Figure 2b) where the Stark effect strongly modulates the  $S_0$ - $S_1$  excitation energy. In principle, for some of the laser intensities used in the simulations, multiphoton excitation to high-lying excited states and photoionization could occur but frozen-nuclei simulations modeling the photoexcitation and photoionization dynamics indicate that these processes are not dominant for the

ultrashort near-single-cycle pulses considered here (see Supporting Information).

We reproduce *in silico* the complete experiment: (i) photoexcitation by the pulse, (ii) nonadiabatic relaxation toward the ground state, and (iii) ground-state dynamics. We used the newly introduced eXternal Field *Ab Initio* Multiple Spawning<sup>42,43</sup> (XFAIMS) method to model the light-matter interaction and nonadiabatic dynamics and Born-Oppenheimer molecular dynamics for the ground-state dynamics (see Supporting Information). In a nutshell, XFAIMS is a trajectory-guided method based on AIMS<sup>44,45</sup> in which nuclear basis functions are propagated classically on the electronic states. Their amplitudes are obtained by integrating the time-dependent Schrödinger equation with the time-dependent molecular Hamiltonian that includes the coupling with the electric field as well as the nonadiabatic couplings. Therefore, XFAIMS accounts for both the Stark shift and field-induced electronic-state mixing. In the simulations, the molecules are oriented and we used a Gaussian shaped pulse whose electric field  $\mathbf{E}(t)$  is defined from the derivative of the vector potential,

$$\mathbf{E}(t) = -\frac{1}{c} \frac{d\mathbf{A}(t)}{dt}, \text{ with } \mathbf{A}(t) \text{ defined as}$$

$$\mathbf{A}(t) = -\frac{\epsilon f_0}{\omega} \exp(-(t-t_0)^2/(2\sigma^2)) \sin(\omega t + \text{CEP})$$

where  $\epsilon$  is the polarization vector,  $f_0$  is the field strength,  $\omega$  is the carrier frequency,  $\sigma$  is related to the pulse duration ( $\text{fwhm} = 2.35\sigma$ ), and CEP is the carrier envelope phase (see the Supporting Information for detailed information).

We first investigate the effect of the CEP for a short and intense 1.7 fs single-cycle pulse polarized at  $45^\circ$  in the  $x$ - $z$  plane (Figure 3). For a CEP that corresponds to a positive maximum of the electric field at the maximum of the pulse envelope (CEP = 0, Figures 1 and 2b), 3% of the population is transferred to  $S_1$ , while for CEP =  $\pi$  the final  $S_1$  population is 2.5 times lower (Figure 3). This is a direct result of the effect of the electric field of the pulse on the electronic energy levels that we can qualitatively rationalize with the Stark effect. The Stark effect lowers the  $S_0$ - $S_1$  excitation energy for CEP = 0

such that the transition becomes more resonant (Figure 2a), while for CEP =  $\pi$ , the excitation energy increases such that the transition becomes strongly off-resonant (Figure 2a), resulting in a reduction of the final  $S_1$  population by more than a factor of 2. For a CEP of  $\pi/2$  and  $3\pi/2$ , the situation differs as the pulse is composed of two maxima (Figure 1), one where the electric field is positive and one where it is negative. Therefore, the  $S_1$  population is the same at the end of the pulse for a CEP of  $\pi/2$  or  $3\pi/2$  but the transient dynamics during the pulse differs as the orientation of the electric field for the first maximum is opposite for the two CEPs (Figure 3a). Once the pulse populates the  $S_1$  state, the wavepacket on  $S_1$  evolves until it reaches a conical intersection<sup>46,47</sup>  $\sim 50$  fs after photoexcitation. This conical intersection connects  $S_1$  to either the ground-state minimum of sulfine (the reactant) or oxathiirane (Figure 1). Then follows a rich hot ground-state dynamics in which eight photoproducts are formed, including dissociated molecules such as  $H_2S$ .<sup>40</sup> The yields of oxathiirane and  $H_2S$  molecules are directly proportional to the  $S_1$  population (Figure 3b) and could be measured by IR spectroscopy,<sup>40</sup> which provides a convenient way to indirectly probe the effect of the CEP.

To unambiguously demonstrate the influence of the Stark effect on the electronic states, we reported the  $S_1$  population for CEP ranging from 0 to  $2\pi$  and for polarization of the laser ranging from  $0^\circ$  to  $45^\circ$  in the  $z-x$  polarization plane (Figure 3c). For a pulse polarized solely in the  $z$  direction ( $0^\circ$ ), there is no Stark effect because the  $S_0$  and  $S_1$  states have no permanent dipole moment along  $z$  due to the  $C_s$  symmetry of the molecule: the  $S_1$  population remains constant, irrespective of the pulse CEP (Figure 3c). When the polarization of the pulse starts to be rotated in the  $x-z$  plane, a larger  $S_1$  population is observed for CEP = 0 than for CEP =  $\pi$ , and this effect further increases as the  $x$ -component of the polarization increases. The maximum of the CEP effect occurs for a polarization of  $45^\circ$ , when the Stark shift induced by the electric field along  $x$  makes the adiabatic excitation energy almost resonant with the laser wavelength (for CEP = 0) and strongly off-resonant (for CEP =  $\pi$ ). It should be noted that the  $S_1$  population is lower for a laser polarization of  $45^\circ$  than  $0^\circ$  because the field strength along the photoexcitation direction  $z$  also decreases.

The laser intensity also alters the effect of the CEP on population transfer, as the Stark shift is directly proportional to electric field of the pulse. For instance, very low field strengths do not lead to a significant variation of the  $S_1$  population as a function of the pulse CEP, while this effect increases with the field strength (Figure 4 and Supporting Information). It should also be noted that the effect of the CEP highlighted here relies on the orientation of the molecule and on the single or near-single-cycle nature of the pulse that ensures that the electric field of the pulse can be oriented either parallel or antiparallel to the molecule when their interaction is the greatest. For longer pulses containing several cycles, the electric field will oscillate between being parallel and antiparallel to the molecule, attenuating (possibly completely) the CEP effect. However, pulses can now contain as few as 1.2 cycles.<sup>20</sup>

In this Letter, we showed that the Stark effect induced by few-cycle pulses can strongly modulate the electronic states PES and should therefore be accounted for when using ultrashort strong pulses. More specifically, we discussed how photoexcitation to the  $S_1$  excited state of the  $H_2CSO$  sulfine can be tailored using CEP-controlled near-single-cycle pulses. The effect of the CEP on the photoexcitation can be

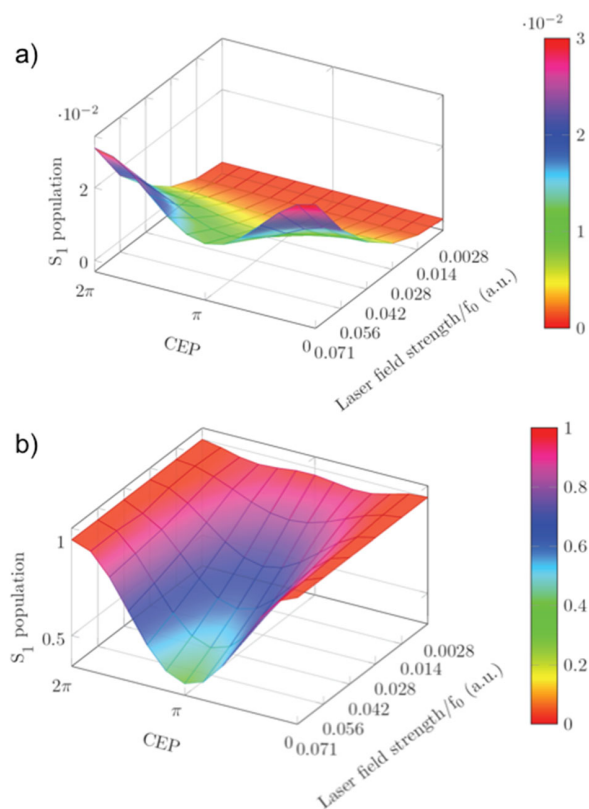


**Figure 4.** (a) Population of the  $S_1$  excited state as a function of the CEP and field strength  $f_0$  for a single-cycle pulse polarized at  $45^\circ$  in the  $x-z$  plane (fwhm = 1.7 fs,  $\omega = 0.063$  au,  $\epsilon = (1/\sqrt{2}, 0, 1/\sqrt{2})$ ). (b) Populations in panel a normalized with respect to the population for CEP = 0, for each field strength, to emphasize the difference of transferred population for CEP = 0 and CEP =  $\pi$ .

rationalized by the simple picture of a pulse-induced Stark effect. By tuning the field strength of the pulse, we can tailor the Stark shift of the  $S_0$  and  $S_1$  electronic states such that, during the pulse, their excitation energy corresponds to the carrier wavelength of the pulse for one value of the CEP. For other values of the CEP, the pulse is off-resonant and the population transferred to the  $S_1$  state is lowered. The sulfine molecule is a textbook case because the transition dipole moment is perpendicular to permanent dipole moments due to symmetry, which allows disentangling the Stark effect from the photoexcitation. Even without this symmetry property, this scheme could be applied to a vast variety of molecules that can be oriented with nonzero permanent dipole moments. The ability to tune excitation energies can be seen as a stepping stone in the tuning of reaction barriers and further toward the control of chemical reactivity.

## AUTHOR INFORMATION

### Corresponding Authors

\*Benoit Mignolet ([bmignolet@uliege.be](mailto:bmignolet@uliege.be)).

\*Todd J. Martinez ([toddjmartinez@gmail.com](mailto:toddjmartinez@gmail.com)).

### ORCID

Benoit Mignolet: 0000-0003-3746-6544

Basile F. E. Curchod: 0000-0002-1705-473X

Francoise Remacle: 0000-0001-7434-5245

Todd J. Martínez: 0000-0002-4798-8947

### Notes

The authors declare no competing financial interest.

## ACKNOWLEDGMENTS

This work was supported by the AMOS program within the Chemical Sciences, Geosciences and Biosciences Division of the Office of Basic Energy Sciences, Office of Science, US Department of Energy. F.R. and B.M. acknowledge support from the Fonds National de la Recherche Scientifique, Belgium (F.R.S.-FNRS) and from the F.R.S.-FNRS research grants T.0132.16 and J.0012.18. Computational resources have been provided by the Consortium des Equipements de Calcul Intensif (CECI), funded by the F.R.S.-FNRS under Grant No. 2.5020.11. This work also made use of the facilities of the Hamilton HPC Service of Durham University and the XStream computational resource supported by the NSF MRI Program (Grant No. ACI-1429830).

## REFERENCES

- (1) Fried, S. D.; Boxer, S. G. Electric Fields and Enzyme Catalysis. *Annu. Rev. Biochem.* **2017**, *86*, 387–415.
- (2) Lau, V. M.; Pfalzgraff, W. C.; Markland, T. E.; Kanan, M. W. Electrostatic Control of Regioselectivity in Au(i)-Catalyzed Hydroarylation. *J. Am. Chem. Soc.* **2017**, *139*, 4035–4041.
- (3) Warshel, A.; Levitt, M. Theoretical studies of enzymic reactions: dielectric, electrostatic and steric stabilization of the carbonium ion in the reaction of lysozyme. *J. Mol. Biol.* **1976**, *103*, 227–249.
- (4) Sussman, B. J.; Townsend, D.; Ivanov, M. Y.; Stollow, A. Dynamic stark control of photochemical processes. *Science* **2006**, *314*, 278–281.
- (5) Neidel, C.; Klei, J.; Yang, C. H.; Rouzée, A.; Vrakking, M. J. J.; Klünder, K.; Miranda, M.; Arnold, C. L.; Fordell, T.; L'Huillier, A.; Gisselbrecht, M.; Johnsson, P.; Dinh, M. P.; Suraud, E.; Reinhard, P. G.; Despré, V.; Marques, M. A. L.; Lépine, F. Probing Time-Dependent Molecular Dipoles on the Attosecond Time Scale. *Phys. Rev. Lett.* **2013**, *111*, No. 033001.
- (6) Sanz-Sanz, C.; Richings, G. W.; Worth, G. A. Dynamic stark control: model studies based on the photodissociation of IBr. *Faraday Discuss.* **2011**, *153*, 275–291.
- (7) Stapelfeldt, H.; Seideman, T. Colloquium: Aligning molecules with strong laser pulses. *Rev. Mod. Phys.* **2003**, *75*, 543.
- (8) Kraus, P. M.; Baykusheva, D.; Wörner, H. J. Two-pulse field-free orientation reveals anisotropy of molecular shape resonance. *Phys. Rev. Lett.* **2014**, *113*, No. 023001.
- (9) Spanner, M.; Patchkovskii, S.; Frumker, E.; Corkum, P. Mechanisms of Two-Color Laser-Induced Field-Free Molecular Orientation. *Phys. Rev. Lett.* **2012**, *109*, 113001.
- (10) Krausz, F.; Ivanov, M. Attosecond physics. *Rev. Mod. Phys.* **2009**, *81*, 163–234.

(11) Nisoli, M.; Decleva, P.; Calegari, F.; Palacios, A.; Martín, F. Attosecond Electron Dynamics in Molecules. *Chem. Rev.* **2017**, *117*, 10760–10825.

(12) Calegari, F.; Sansone, G.; Stagira, S.; Vozzi, C.; Nisoli, M. Advances in attosecond science. *J. Phys. B: At, Mol. Opt. Phys.* **2016**, *49*, No. 062001.

(13) Hentschel, M.; Kienberger, R.; Spielmann, C.; Reider, G. A.; Milosevic, N.; Brabec, T.; Corkum, P.; Heinzmann, U.; Drescher, M.; Krausz, F. Attosecond metrology. *Nature* **2001**, *414*, 509–513.

(14) Sansone, G.; Benedetti, E.; Calegari, F.; Vozzi, C.; Avaldi, L.; Flammini, R.; Poletto, L.; Villoresi, P.; Altucci, C.; Velotta, R. Isolated single-cycle attosecond pulses. *Science* **2006**, *314*, 443–446.

(15) Hauri, C. P.; Kornelis, W.; Helbing, F. W.; Heinrich, A.; Couairon, A.; Mysyrowicz, A.; Biegert, J.; Keller, U. Generation of intense, carrier-envelope phase-locked few-cycle laser pulses through filamentation. *Appl. Phys. B: Lasers Opt.* **2004**, *79*, 673–677.

(16) Chen, W.-J.; Hsieh, Z.-M.; Huang, S. W.; Su, H.-Y.; Lai, C.-J.; Tang, T.-T.; Lin, C.-H.; Lee, C.-K.; Pan, R.-P.; Pan, C.-L. Sub-single-cycle optical pulse train with constant carrier envelope phase. *Phys. Rev. Lett.* **2008**, *100*, 163906.

(17) Nisoli, M.; De Silvestri, S.; Svelto, O.; Szpöcs, R.; Ferencz, K.; Spielmann, C.; Sartania, S.; Krausz, F. Compression of high-energy laser pulses below 5 fs. *Opt. Lett.* **1997**, *22*, 522–524.

(18) Süßmann, F.; Zharebtsov, S.; Plenge, J.; Johnson, N. G.; Kübel, M.; Saylor, A. M.; Mondes, V.; Graf, C.; Rühl, E.; Paulus, G. G. Single-shot velocity-map imaging of attosecond light-field control at kilohertz rate. *Rev. Sci. Instrum.* **2011**, *82*, No. 093109.

(19) Johnson, N. G.; Herrwerth, O.; Wirth, A.; De, S.; Ben-Itzhak, I.; Lezius, M.; Bergues, B.; Kling, M. F.; Senfleben, A.; Schröter, C. D. Single-shot carrier-envelope-phase-tagged ion-momentum imaging of nonsequential double ionization of argon in intense 4-fs laser fields. *Phys. Rev. A: At, Mol., Opt. Phys.* **2011**, *83*, No. 013412.

(20) Timmers, H.; Kobayashi, Y.; Chang, K. F.; Reduzzi, M.; Neumark, D. M.; Leone, S. R. Generating high-contrast, near single-cycle waveforms with third-order dispersion compensation. *Opt. Lett.* **2017**, *42*, 811–814.

(21) Shverdin, M. Y.; Walker, D. R.; Yavuz, D. D.; Yin, G. Y.; Harris, S. E. Generation of a single-cycle optical pulse. *Phys. Rev. Lett.* **2005**, *94*, No. 033904.

(22) Paulus, G. G.; Grasbon, F.; Walther, H.; Villoresi, P.; Nisoli, M.; Stagira, S.; Priori, E.; De Silvestri, S. Absolute-phase phenomena in photoionization with few-cycle laser pulses. *Nature* **2001**, *414*, 182–184.

(23) Baltuška, A.; Udem, T.; Uiberacker, M.; Hentschel, M.; Goulielmakis, E.; Gohle, C.; Holzwarth, R.; Yakovlev, V. S.; Scrinzi, A.; Hänsch, T. W. Attosecond control of electronic processes by intense light fields. *Nature* **2003**, *421*, 611–615.

(24) Schiffrin, A.; Paasch-Colberg, T.; Karpowicz, N.; Apalkov, V.; Gerster, D.; Muhlbrandt, S.; Korbman, M.; Reichert, J.; Schultze, M.; Holzner, S.; Barth, J. V.; Kienberger, R.; Ernstorf, R.; Yakovlev, V. S.; Stockman, M. I.; Krausz, F. Optical-field-induced current in dielectrics. *Nature* **2012**, *493*, 70–74.

(25) Kling, M. F.; von den Hoff, P.; Znakovskaya, I.; de Vivie-Riedle, R. (Sub-) femtosecond control of molecular reactions via tailoring the electric field of light. *Phys. Chem. Chem. Phys.* **2013**, *15*, 9448–9467.

(26) Sansone, G.; Kelkensberg, F.; Pérez-Torres, J. F.; Morales, F.; Kling, M. F.; Siu, W.; Ghafur, O.; Johnsson, P.; Swoboda, M.; Benedetti, E. Electron localization following attosecond molecular photoionization. *Nature* **2010**, *465*, 763–766.

(27) Kling, M. F.; Siedschlag, C.; Verhoef, A. J.; Khan, J. I.; Schultze, M.; Uphues, T.; Ni, Y.; Uiberacker, M.; Drescher, M.; Krausz, F. Control of electron localization in molecular dissociation. *Science* **2006**, *312*, 246–248.

(28) Znakovskaya, I.; von Den Hoff, P.; Zharebtsov, S.; Wirth, A.; Herrwerth, O.; Vrakking, M. J. J.; de Vivie-Riedle, R.; Kling, M. F. Attosecond control of electron dynamics in carbon monoxide. *Phys. Rev. Lett.* **2009**, *103*, 103002.

(29) Liu, Y.; Liu, X.; Deng, Y.; Wu, C.; Jiang, H.; Gong, Q. Selective steering of molecular multiple dissociative channels with strong few-cycle laser pulses. *Phys. Rev. Lett.* **2011**, *106*, No. 073004.

(30) Znakovskaya, I.; Von den Hoff, P.; Schirmel, N.; Urbasch, G.; Zherebtsov, S.; Bergues, B.; de Vivie-Riedle, R.; Weitzel, K. M.; Kling, M. F. Waveform control of orientation-dependent ionization of DCl in few-cycle laser fields. *Phys. Chem. Chem. Phys.* **2011**, *13*, 8653–8658.

(31) Kübel, M.; Siemering, R.; Burger, C.; Kling, N. G.; Li, H.; Alnaser, A. S.; Bergues, B.; Zherebtsov, S.; Azzeer, A. M.; Ben-Itzhak, I. Steering proton migration in hydrocarbons using intense few-cycle laser fields. *Phys. Rev. Lett.* **2016**, *116*, 193001.

(32) Alnaser, A. S.; Kübel, M.; Siemering, R.; Bergues, B.; Kling, N. G.; Betsch, K. J.; Deng, Y.; Schmidt, J.; Alahmed, Z. A.; Azzeer, A. M., Subfemtosecond steering of hydrocarbon deprotonation through superposition of vibrational modes. *Nat. Commun.* **2014**, *5*, 3800

(33) Xie, X.; Doblhoff-Dier, K.; Roither, S.; Schöffler, M. S.; Kartashov, D.; Xu, H.; Rathje, T.; Paulus, G. G.; Baltuška, A.; Gräfe, S.; Kitzler, M. Attosecond-Recollision-Controlled Selective Fragmentation of Polyatomic Molecules. *Phys. Rev. Lett.* **2012**, *109*, 243001.

(34) Li, H.; Mignolet, B.; Wachter, G.; Skruszewicz, S.; Zherebtsov, S.; Süßmann, F.; Kessel, A.; Trushin, S. A.; Kling, N. G.; Kübel, M.; Burgdörfer, J.; Levine, R. D.; Remacle, F.; Kling, M. Coherent electronic wave packet motion in C<sub>60</sub> controlled by the waveform and polarization of few-cycle laser fields. *Phys. Rev. Lett.* **2015**, *114*, 123004.

(35) Remacle, F.; Nest, M.; Levine, R. D. Laser steered ultrafast quantum dynamics of electrons in LiH. *Phys. Rev. Lett.* **2007**, *99*, 183902–4.

(36) Mignolet, B.; Gijsbertsen, A.; Vrakking, M. J. J.; Levine, R. D.; Remacle, F. Stereocontrol of attosecond time-scale electron dynamics in ABCU using ultrafast laser pulses: a computational study. *Phys. Chem. Chem. Phys.* **2011**, *13*, 8331–8344.

(37) Kamta, G. L.; Bandrauk, A. D. Phase dependence of enhanced ionization in asymmetric molecules. *Phys. Rev. Lett.* **2005**, *94*, 203003.

(38) Nikodem, A.; Levine, R. D.; Remacle, F. Spatial and temporal control of populations, branching ratios, and electronic coherences in LiH by a single one-cycle infrared pulse. *Phys. Rev. A: At, Mol, Opt. Phys.* **2017**, *95*, No. 053404.

(39) Remacle, F.; Levine, R. D. Attosecond pumping of nonstationary electronic states of LiH: Charge shake-up and electron density distortion. *Phys. Rev. A: At, Mol, Opt. Phys.* **2011**, *83*, No. 013411.

(40) Mignolet, B.; Curchod, B. F. E.; Martínez, T. J. Rich Athermal Ground-State Chemistry Triggered by Dynamics through a Conical Intersection. *Angew. Chem., Int. Ed.* **2016**, *55*, 14993–14996.

(41) Schreiner, P. R.; Reisenauer, H. P.; Romanski, J.; Mloston, G. Oxathiirane. *J. Am. Chem. Soc.* **2010**, *132*, 7240–7241.

(42) Mignolet, B.; Curchod, B. F. E.; Martínez, T. J. XFAIMS-eXternal Field Ab Initio Multiple Spawning for electron-nuclear dynamics triggered by short laser pulses. *J. Chem. Phys.* **2016**, *145*, 191104.

(43) Mignolet, B.; Curchod, B. F. E. A walk through the approximations of ab initio multiple spawning. *J. Chem. Phys.* **2018**, *148*, 134110.

(44) Martínez, T. J.; Ben-Nun, M.; Levine, R. D. Multi-Electronic-State Molecular Dynamics: A Wave Function Approach with Applications. *J. Phys. Chem.* **1996**, *100*, 7884–7895.

(45) Curchod, B. F. E.; Martínez, T. J. Ab Initio Nonadiabatic Quantum Molecular Dynamics. *Chem. Rev.* **2018**, *118*, 3305–3336.

(46) Bernardi, F.; Olivucci, M.; Robb, M. A. Potential energy surface crossings in organic photochemistry. *Chem. Soc. Rev.* **1996**, *25*, 321–328.

(47) Domcke, W.; Yarkony, D. *Conical intersections: electronic structure, dynamics & spectroscopy*. World Scientific: 2004; Vol. 15.